Transactions, SMiRT-22
San Francisco, California, USA - August 18-23, 2013
Division IX (include assigned division number from I to X)

DYNAMIC SIMULATIONS FOR THE SEISMIC BEHAVIOR OF THE FAULT PLANE IN THE SUBDUCTION ZONE DURING MEGA-THRUST EARTHQUAKES

T Osaki[1], S Iwase[1], H Uratani[1], K Tsuda[2], K Dan[2], K Irie[2], S Dorjpalam[2], S Ogawa[2], and T Watanabe[2]

[1] Chubu Electric Power Co., Inc., Aichi, JAPAN
[2] Ohsaki Research Institute, Inc, Tokyo, JAPAN
E-mail of corresponding author: Osaki.Takashi@chuden.co.jp

ABSTRACT

In order to improve the seismic safety of nuclear facilities, the ground motion predictions reflecting the seismic behavior of the fault plane are necessary. One of the most notable features observed in the recent mega-thrust earthquakes, such as the 2011 Tohoku-Oki earthquake, is that the shallow part of the fault plane produced large slips on the order of several ten meters without radiating strong ground motions (e.g. Lay et al., 2012). Thus, reflecting this feature on the ground motion prediction is important.

In this study, we carried out the dynamic simulations in order to understand the seismic behavior of the fault plane during mega-thrust earthquakes. We used the two-dimensional spectral element method (Ampuero, 2009) that can incorporate the complex fault geometry into simulation as well as save computational resources. The simulation utilizes the slip-weakening law (Ida, 1972). In the simulation, we investigated the seismic behavior by changing the values of parameters, such as stress drop, material parameters and critical slip distance (Dc) and the rupture directivity. The results of simulations may also be applicable to understand the seismic behavior of the fault plane during the future mega-thrust earthquakes e.g., along the Nankai Trough, Japan.

INTRODUCTION

In the seismic design of the nuclear facilities in Japan, the ground motion predictions for a target site are necessary. These ground motion predictions have been achieved based on the response spectra (e.g., Hisada et al., 1978; Noda et al., 2002) that use the magnitude and distance of the target earthquakes for a long time. On the other hand, recent studies showed that ground motion prediction with the source fault simulated successfully the observed data after the 1995 Kobe earthquake. This led to the adoption of the multiple ground motion prediction methods based on the source fault model in addition to the response spectra for the nuclear facilities in Japan (Nuclear Safety Commission of Japan, 2006).

In order to predict ground motions, the features of seismic behavior of source fault that might affect the ground motions need to be captured. The analysis of the observed data by the recent large crustal earthquakes revealed that the strong ground motions (short-period ground motions) are radiated from some specific area called Strong Motion Generation Area (SMGA, hereafter), not from entire fault plane (Irikura and Miyake, 2001). Since then, the source fault models with SMGA are used for the strong ground motion predictions. The seismic source fault models with SMGA assume that the large slip area also radiate the strong ground motion (e.g., The Headquarters for Earthquake Research Promotion, 2007) and the shallow part of the fault plane with soft material does not radiate the strong ground motions.

Recent Mega-Thrust Earthquakes

The observations from the recent mega-thrust earthquakes, however, indicate that the SMGA should be modeled separately from the large slip area. The analysis of observed data from the 2011

Tohoku-Oki earthquake (Tohoku earthquake, hereafter), that is the mega-thrust earthquake caused by the seismic fault on the plate boundary, revealed that large slips on the order of several ten meters are produced on the shallow part of fault plane (close to the trench) and strong ground motions (are radiated from the deeper part of the fault plane (landward), not from the shallow part of the fault plane with large slips (e.g., Kurahashi and Irikura, 2011; Yoshida et al., 2011). Figure 1(a) shows the examples of the slip distribution of the Tohoku earthquake (Yoshida et al., 2011) and the location of SMGA depicted by Kurahashi and Irikura (2011). This feature has also been recognized by the recent mega-thrust earthquakes such as 2004 Sumatra earthquake. Figure 1(b) and (c) show the estimated area with radiating short-period ground motions (Blue) and that with long-period ground motions (Yellow) for the Tohoku earthquake (b) and Sumatra earthquake (c) extracted by Lay et al. (2012). These observations are not consistent with the idea for the source fault model that the large slip area assumes to radiate also strong ground motions, but follow the idea that the strong ground motions are not radiated from the shallow part of the fault plane. This seismic behavior of the fault plane is thought to be the typical features of the mega-thrust earthquakes that the rupture reaches to the shallow part of the fault plane, and thus understanding these features is important for the future ground motion predictions.

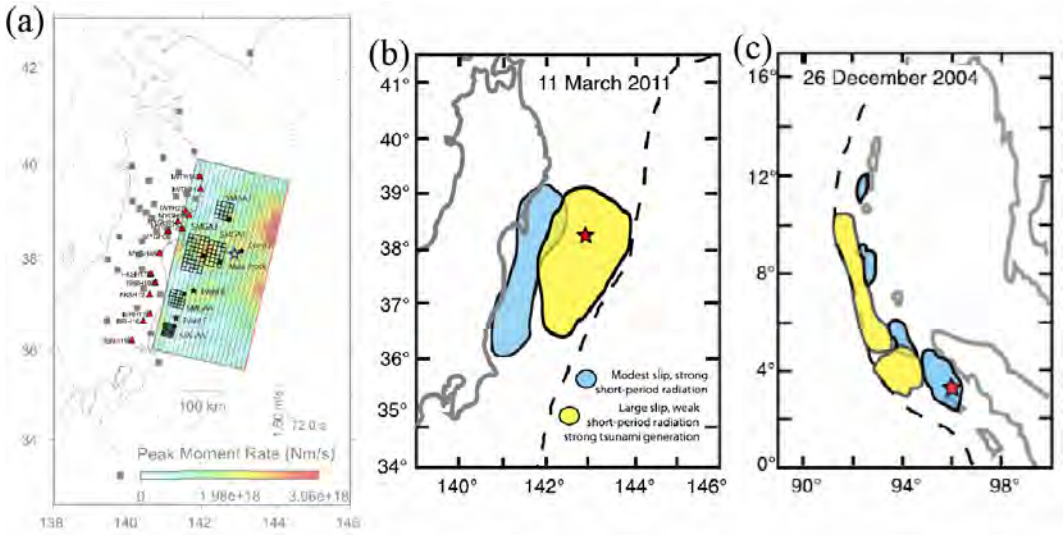

Figure 1 (a) Source model of the 2011 Tohoku earthquake proposed by Kurahashi and Irikura (2011) considering SMGA. The five SMGAs are superposed on the distribution of peak moment-rate inverted using strong motion data by Yoshida et al. (2011).Schematic summary of patterns of coherent short-period radiation and large seismic slip areas for the Tohoku earthquake (b) and 2004 Sumatra earthquake (c) (Lay et al., 2012).

This Study

Based on the idea for the mega-thrust earthquakes mentioned above, we built the conceptual images of the seismic behavior for the rupture of mega-thrust earthquake as shown in Figure 2. The fault plane of the mega-thrust earthquake might be classified into three areas based on its property of the fault plane: (i) Deeper part with radiating strong ground motions (SMGA) (ii) Deeper part with small slip without radiating strong ground motions (Background area), and (iii) Shallow part of the fault plane producing large slip (Large Slip Area) without radiating strong ground motions. Each area has different distinct features in terms of the state of plate-coupling i.e., the strength of fault plane as well as the degree of stress drops. These differences lead to the different features of seismic behavior. The shallow part of the fault plane (Large Slip Area (iii) in Figure 2) was originally thought to rupture slowly during the mega-thrust earthquakes.

In this study, we have tried to understand the seismic behavior of the fault plane during the mega-thrust earthquakes based on the dynamic simulations. The dynamic simulation is able to examine the seismic behavior of the fault plane *i.e.,* how the rupture evolves with the proper initial conditions. We changed the values of parameters controlling seismic behavior of the fault plane, such as stress drop, material property, and critical slip distance (Dc) and the rupture directivity to make discussions about how these parameters affect the seismic behavior of the fault plane and how the ground motion changes within the framework of the current seismic source fault model. We built two series of the models and grouped them based on 1) the heterogeneity of stress drop and 2) the parameter variations on the shallow part with assuming homogeneous stress drop. Then we examined the feature of the seismic behavior of the fault plane for each group. Even though the model we constructed is simple, the results of the simulations are useful to understand the seismic behavior of the fault plane during the future mega-thrust earthquakes e.g., along the Nankai Trough, Japan.

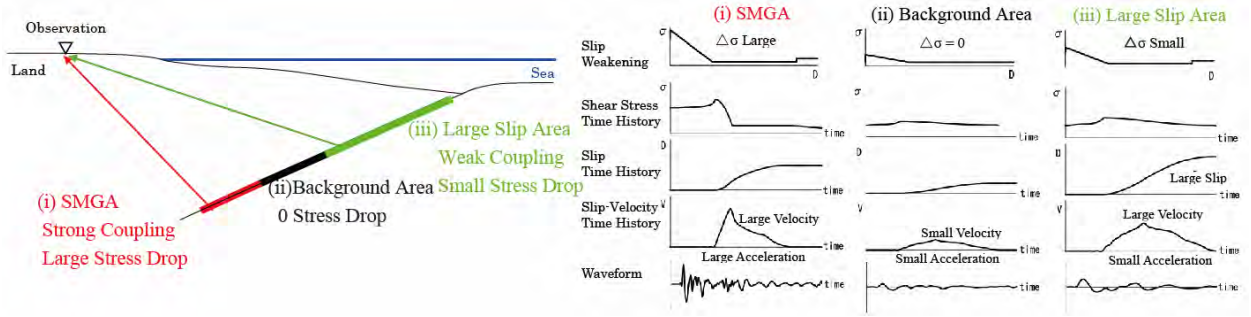

Figure 2 Conceptual illustration of seismic behavior on the fault plane of mega-thrust earthquakes (left). Each area shows some features of time histories of the corresponding parameters based on the property of fault plane (state of plate coupling and stress drop).

SIMULATION CONDITION

Method

In this study, we have used the two-dimensional spectral-element method (Ampuero, 2009) for the simulation. This method can incorporate the complex fault geometry into simulation and save computational resources compared to the conventional finite-element method. We set the model of 650 km (horizontal) long x 200 km (vertical) wide in order to reduce the effects of reflected waves from the boundary as much as possible. The mesh used for the simulation is shown in Figure 3. The medium property is set homogeneous. The red line in Figure 3 corresponds to the fault plane assuming the Kelvin-Voigt material introduced to remove the short-period artificial oscillations. The linear elastic body is assumed for other medium. We utilize the free surface condition on the surface and set the absorbing boundary condition for other boundaries.

A linear slip-weakening friction law (Ida, 1972) is employed on the fault plane with dipping 15 degrees imaging the Nankai Trough. In this friction law, the shear stress is a function of slip. After the slip initiates on the yielding stress σ^y representing via normal stress σ^N and static frictional coefficient μ_s, the stress decreases linearly to the dynamic frictional stress σ^f ($= \mu_d \cdot \sigma^N$, μ_d: dynamic frictional coefficient) over the critical slip distance (Dc) and keeps the dynamic frictional stress level until slip ends (Figure 4). The difference between σ^y and initial shear stress σ^o is called the strength excess (SE) controlling the rupture initiation and the stress drop ($\Delta\sigma$) defines the difference between σ^o and σ^f (Figure 4). The parameter for the simulation is listed on the Table 1. The value of stress drop is set 3MPa for the averaged values of the inter-plate earthquake (Kanamori and Anderson, 1975). The medium is assumed to be homogeneous and the slip-strengthening area is assumed on the deeper (deeper than 40 km) part of the model. The slip-strengthening friction is assumed that the dynamic stress is bigger than yield stress to

prevent from producing slip on the fault plane on the deeper part. In a real case of subduction zone, the depth of slip-strengthening area (40 km in this model) might be considered as the lower-limit of seismogenic zone.

Table 1 Parameters for simulation

Model Area	650 km (horizontal) x 200 km (vertical)
Medium Parameter	Vs =3.54 km/s, Vp = 6.3 km/s, ρ =2.76g/cm^3
Dip Angle	15°
Average Stress Drop	3 MPa (Kanamori and Anderson, 1975)
Frictional Parameters	0.6 (static frictional coefficient μ_s) 0.2 (dynamic frictional coefficient μ_d)
Dc	0.5 m
Slip-Strengthening Area	Deeper than 40 km on the fault

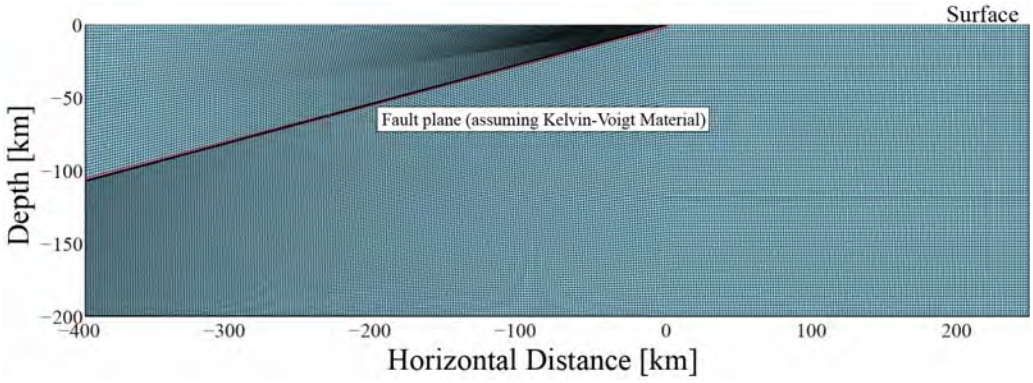

Figure 3 Mesh used for the calculation

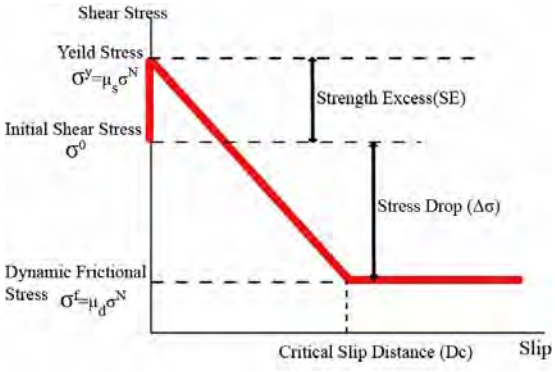

Figure 4 Slip-weakening friction law used in this study (Ida, 1972)

Simulation Model

The seismic behaviors of the fault plane are usually controlled by the combinations of several parameters, such as stress drop, Dc, rupture directivity etc. This indicates that estimating how each parameter affects the seismic behavior separately is very important to understand the seismic behaviors of the fault plane. In this study, we set five models (here after calling Model A through Model E) to investigate the effects of parameters on the seismic behavior of fault plane. Model A is the basic model with homogeneous parameters (stress drop distribution, Dc, material properties) listed in Table 1.

Model B and Model C are set to investigate the difference of the area for producing large slip and SMGA on the fault plane. Model B and Model C have the area with large stress drop (Δσ) on the fault plane. The area with large Δσ (Table 2) is expected to produce more short-period ground motions from it. The other conditions except Δσ variations are the same as Model A. The location of nucleation zone is put below the large Δσ area in Model B and the locations of large Δσ area and nucleation zone are reversed in Model C (Table 2, Figure 5(1)) to investigate how the rupture directivity controls rupture evolution.

Then we set the models to investigate the effects of parameters of the shallow part of the models with assuming homogeneous stress drop. Because the material property near the surface is one of the important parameters to control the level of ground motions, we first put the layer of soft material near the surface (Table 2) up to 10 km depth (Figure 5(2)) in Model D. The simulation condition is the same as Model A except this material property near the surface. Another parameter we change is Dc which is important parameter for ground motion prediction on the seismic behavior. Dc controls the shape of the onset of slip-rate functions and how shear stress is changed until it reaches to the dynamic frictional stress (Figure 4). In this study, large Dc value (Table 2) is put on the area near the surface (shallower than 10 km, Figure 5(2)) and the other conditions except Dc near the surface is the same as Model A. The detail of how the parameter has been changed is described on Table 2. The features of each model are shown in Figure 5. In this study, we show the results for each pair(Model B and Model C as the Stress Drop Variation and Model D and Model E as the Shallow Parameter Variation).

Table2 Parameter Combination for the Simulation

Model	Δσ	Dc	Medium	Note (How the Parameters Have Been Changed)
A	Uniform	Uniform	Homogeneous	
B	Variable	Uniform	Homogeneous	Set Areas with Large (6MPa) Stress Drop (= SMGA) and 0 Stress Drop (= Background)
C	Variable	Uniform	Homogeneous	Locations of Nucleation Zone and Asperity are Reversed to those of Model B
D	Uniform	Uniform	2-Layer	Vp 4.47 km/s Vs 2.47 km/s (Shallower than 10 km), Vp 6.3 km/s Vs 3.54 km/s (Otherwise)
E	Uniform	Variable	Homogeneous	Dc = 3.0 m (Shallower than 10 km) , 0.5 m (Otherwise)

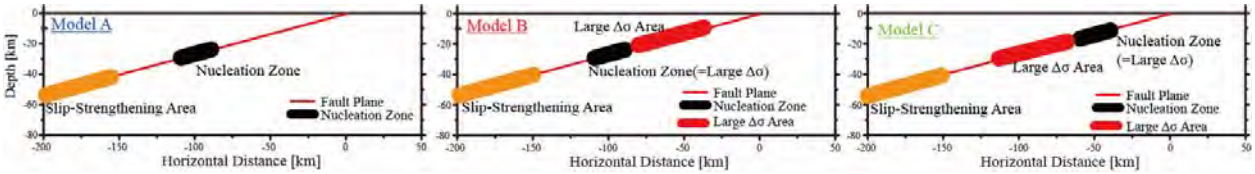

(1) Model Settings for the Stress Drop Variations (Δσ)

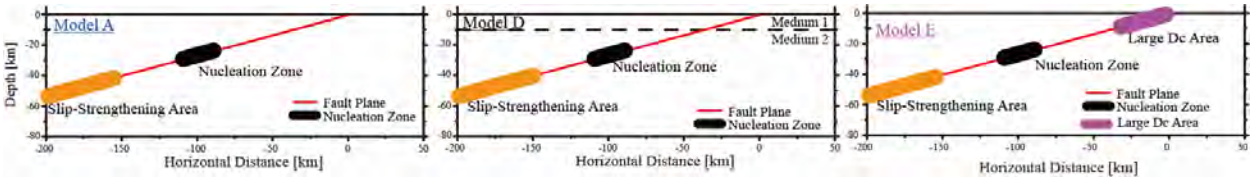

(2) Model Settings for the Shallow (shallower than 10km depth) Parameter Variations

Figure 5 Simulation conditions of each model (magnifying the shallow part of the model of Figure 3)

Based on five models described above, we made a comparison between two models to investigate the effects of each parameter (Table 2) on the seismic behavior in each group. Each comparison is made based on the slip distribution (how the slip evolves as a function of time) and the time histories of slip-rate function and slip-acceleration function especially on the shallow part of the fault plane. And then in order to investigate more detail about how the feature of seismic behavior changes with depth, we have compared the distribution of peak values for each comparison as a function of depth. We consider the final slip as representing long-period ground motion, and the values of peak slip acceleration as representing short-period ground motion, respectively. We have made the discussion about the feature of

the distribution of final slip and values of peak slip acceleration as a function of depth following the results of each model.

STRESS DROP VARIATION

Results

The results with putting large stress drop (Δσ) above the nucleation zone (Figure 5(1)) in Model B are shown in Figure 6 in comparison with the results of Model A. The final slip is similar between these two models shown in Figure 6(1) except the area with large Δσ in Model B around 10-25 km depth. This difference leads to the steep arrival of slip-velocity functions (Figure 6 (2)) and large amplitude of slip-acceleration functions shown in Figure 6(3) on the area with large Δσ (rectangle area in Figure 6(2) and (3)).

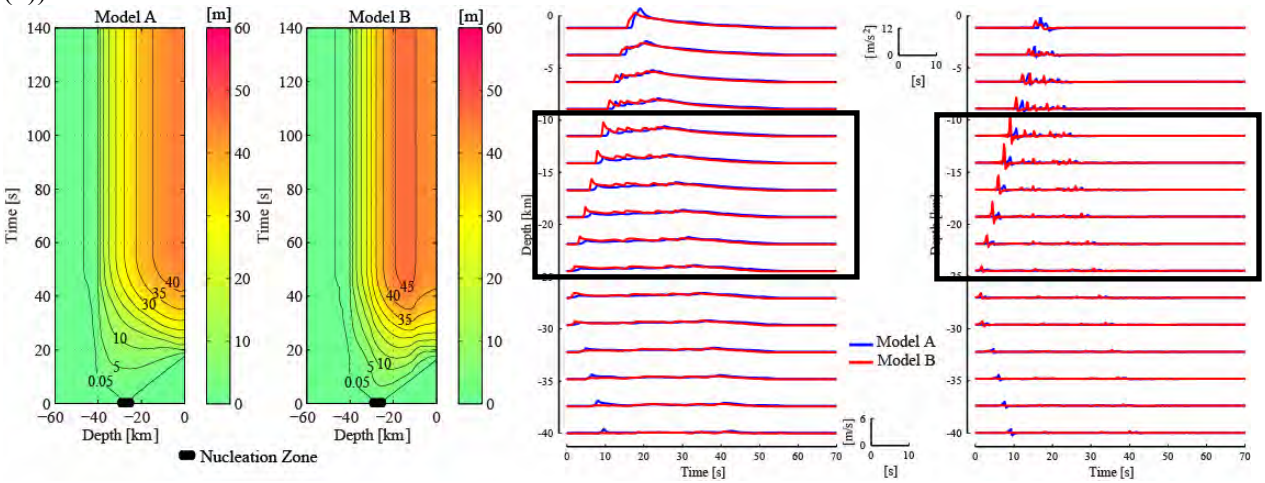

(1) Slip distribution (2) Slip-Rate function (3) Slip-Acceleration function

Figure 6 Comparison of the simulation results for Model A and Model B

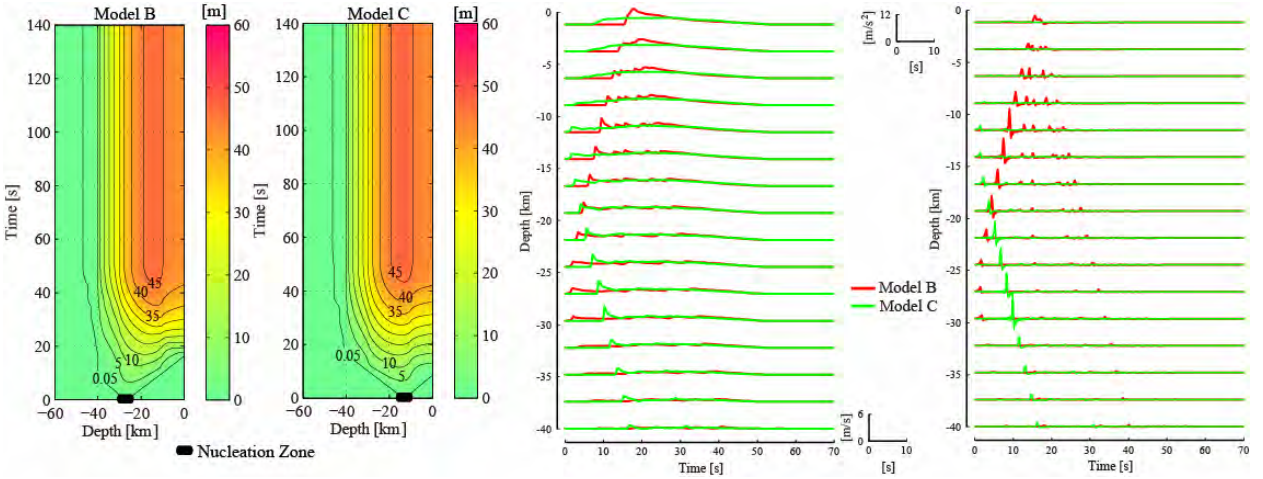

(1) Slip distribution (2) Slip-Rate function (3) Slip-Acceleration function

Figure 7 Comparison of the simulation results for between Model B and Model C

The area with large slip as well as large amplitudes of slip-velocity and slip-acceleration corresponds to the area with large Δσ. This follows the assumption by the seismic fault source model with SMGA with

large Δσ, and this model was originally used for the ground motion predictions. The detail features of the distribution of peak values (slip and peak-slip acceleration) are discussed later.

The comparisons of the simulation results for Model B and C (how the rupture directivity affects the rupture evolution) are shown in Figure 7. Even the rupture directivity is opposite for two models, the slip distribution (Figure 7(1)) is same. The slip-rate function (Figure 7(2)) and the slip-acceleration function (Figure 7(3)) reflect the rupture directivity for each model. The pulse propagating up-wards of Model C has much less amplitude near the surface compared to it of Model B, and the depth where the pulse shows the large amplitude of Model C is deeper than that of Model B.

Discussion

We show the distribution of final slip and peak-slip acceleration as a function of depth for each comparison in Figure 8. The rapid increase of peak slip acceleration values close to the surface (the area shallower than 2-3 km depth) may be caused by the shallow dipping angle and the free surface conditions (Ma and Beroza, 2008). Having more discussions about whether this phenomenon actually comes from the real seismic observations will be the future work.

The differences of final slip distribution reflect how the parameter has been changed for the comparison of Model A-Mode B shown as Figure 8(1).

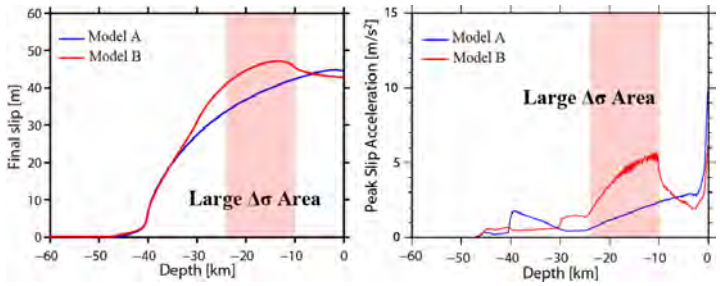

(1) Comparison of Model A and Model B

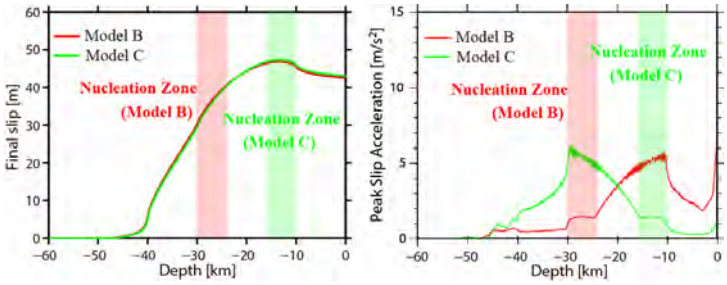

(2) Comparison of Model B and Model C

Figure 8 Final slip distributions (left) and peak slip-acceleration distributions (right) for each comparison

Putting the large Δσ (SMGA) around the area of 10-25 km depth (Red Hatched area in Figure 8(1)) in Model B agrees with the area having larger final slip compared to the area in Model A as well as the large values of peak slip-acceleration. This comparison of Model A-Model B indicates that the result showing the coincidence of the locations between the large Δσ and the large values of the peak slip acceleration as well as the final slip agrees with the assumption of current seismic source fault model that the large slip area also radiates large short-period ground motions.

The effects of rupture directivity is little when the final slip distribution of Model B-Model C is compared shown as Figure 8(2). On the contrary, the distributions of peak slip acceleration of Model C show that the backward direction on the shallow part of the fault plane (right hand side of the nucleation

zone of green hatched area in Figure 8(2)) radiates small amount of short-period ground motions compared to Model B.

Even no observations have been reported that short period ground motions are radiated from the shallow part of the fault so far, this trend of Model C with SMGA (large stress drop area) on the deeper part of the fault plane and assumed the rupture direction from shallow to deep, showing large slip without radiating short-period ground motions on the shallow part of fault plane, was similar to that of the mega-thrust earthquakes described in Lay et al. (2012) (Figure 1(b) , (c)).

SHALLOW PARAMTER VARIATION

Results

We show the comparison between Model A and Model D with soft material layer in Figure 9. The slip amplitude (Figure 9(1)) and amplitude of slip-rate functions (Figure 9(2)) are not only amplified above the depth of material contrast but the amplitudes of slip-acceleration (Figure 9(3)) above 10 km depth are also amplified.

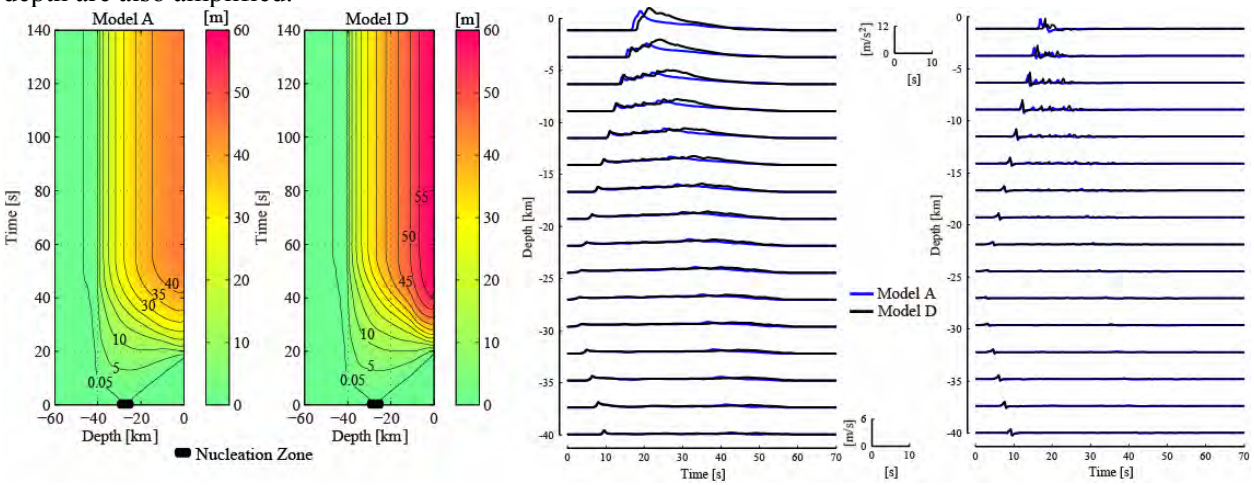

(1) Slip distribution (2) Slip-Rate function (3) Slip-Acceleration function

Figure 9 Comparison of the simulation results for between Model A and Model D

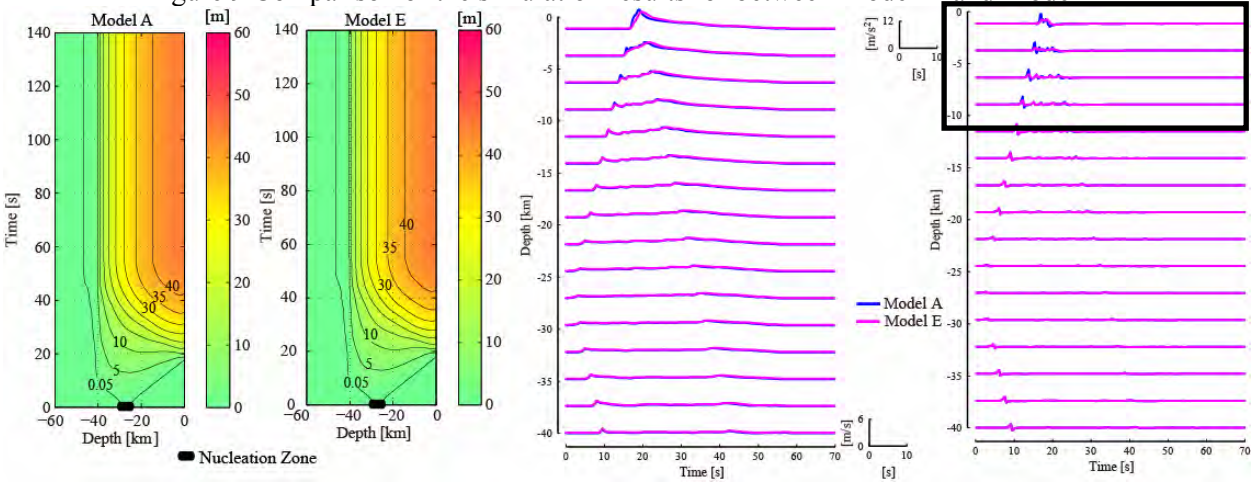

(1) Slip distribution (2) Slip-Rate function (3) Slip-Acceleration function

Figure 10 Comparison of the simulation results for between Model A and Model E

The comparisons between Model A and Model E that puts large Dc area near the surface are shown in Figure 10. The amplitude of slip-acceleration near the surface with large Dc rectangle area in Figure 10(3) is getting smaller shown in Figure 10(3). This trend agrees with what Tsuda et al. (2012) mentioned that the large Dc value (Model E) might cause the reduction of amplitude of short-period ground motions. This indicates the speed of rupture is getting slow because of large Dc near the surface. On the other hand, the slip distribution (Figure 10(1)) and the shape of slip-rate function (Figure 10(2)) including its amplitude look similar for two models. This indicates that the variation of Dc has little influence on the radiation for long-period ground motion. The detail features of the distribution of peak values (slip and peak-slip acceleration) are discussed as follows.

Discussion

We show the distribution of final slip and peak slip acceleration as a function of depth for each comparison in Figure 11. The rapid increase of peak slip acceleration values close to the surface is left to the future discussion like the other cases (Figure 8).

The distribution of final slip as well as peak-slip acceleration reflects how the material parameter has been changed for the comparison of Model A-Model D shown in Figure 11(1). This trend indicates that if the layer of soft material exists, the seismic waves radiating from the fault plane is amplified regardless of its period based on the conditions of homogeneous stress drop and constant Dc in Model D.

Putting large Dc on the shallow part has little influence on the final slip distribution shown in Figure 11(2). On the contrary, the large Dc area shallower than 10 km reduces the value of peak slip acceleration within that area compared to that without large Dc area (Model A).

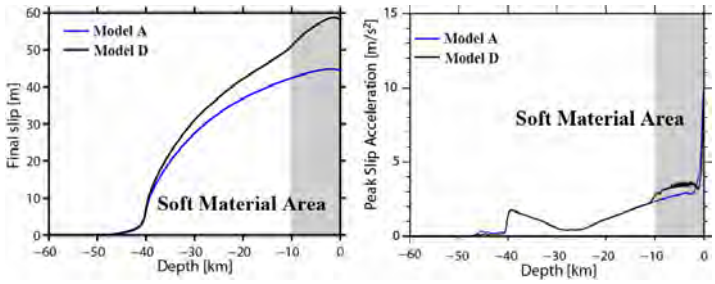

(1) Comparison of Model A and Model D

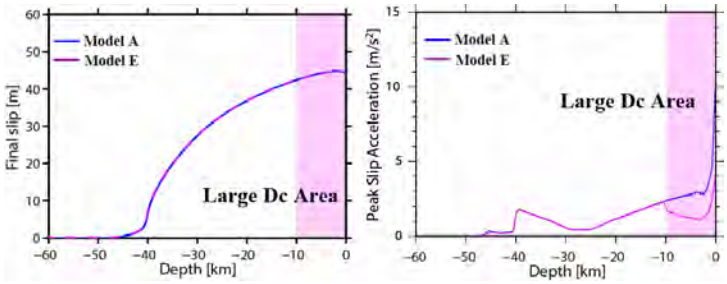

(2) Comparison of Model A and Model E

Figure 11 Final slip distributions (left) and peak slip-acceleration distributions (right) for each comparison

CONCLUSION

We did the dynamic simulations using the simple models imaging mega-thrust earthquakes with changing values of parameters (stress drop, rupture directivity, material properties, and Dc) to understand the seismic behavior of the fault plane.

The model with SMGA (large stress drop area) on the deeper part of the fault plane and assumed the rupture direction from shallow to deep reproduced the general features of the seismic behavior that produce large slip without radiating strong ground motions for the shallow part of the fault plane as seen during the mega-thrust earthquake, such as the Tohoku Earthquake.

In the models with assuming homogeneous stress drop, the values of the material properties and Dc near the surface were varied to examine how the final slip and the peak slip acceleration changed.

The interpretations of these results about how the fault behaves through dynamic simulations with varying parameters enable us to have the understandings of the seismic behavior of the fault plane during the mega-thrust earthquakes.

REFERENCES

Ampuero, J. P. (2009) SEM2DPACK, A Spectral Element Method tool for 2D wave propagation and earthquake source dynamics User's Guide

Hisada, T., Y. Ohsaki, M. Watabe and T. Ohta (1978) Design Spectra for Stiff Structures on Rock, Proceedings of The Second International Conference on Microzonation, Vol. III, Nov.

Ida, Y. (1972) Cohesive force across the tip of a longitudinal-shear crack and Griffith's specific surface energy, J. Geophys. Res., **77**, 3796–3805.

Irikura, K. and H. Miyake (2001), Prediction of strong ground motions for scenario earthquakes, Journal of Geography **110**, 849–875 (in Japanese with English abstract).

Kanamori, H. and D. L. Anderson (1975) Theoretical basis of some empirical relations in seismology: Bull. Seismol. Soc. Am., **65**, 1073-1095

Kurahashi, S. and K. Irikura (2011) Source model for generating strong ground motions during the 2011 off the Pacific coast of Tohoku earthquake, Earth Planets Space, **63**, 571–576

Lay, T., H. Kanamori, C. J. Ammon, K. D. Koper, A. R. Hutko, L. Ye, H. Yue, and T. M. Rushing (2012) Depth-varying rupture properties of subduction zone megathrust faults, J. Geophys. Res., 117, B04311, doi:10.1029/2011JB009133.

Ma, S., and G. C. Beroza (2008) Rupture dynamics on a bi-material interface for dipping faults, *Bull. Seismol. Soc. Am*., **98**, p. 1642-1658

Noda S, K. Yashiro, K. Takahashi, M. Takemura, S. Ohno, M. Tohdo, T. Watanabe (2002) Response spectra for design purpose of stiff structures of rock site, OECS/NEA Workshop, Oct. 2002.

Nuclear Safety Commission of Japan (2006) The Regulatory Guide for Reviewing Seismic Design of Nuclear Power Reactor Facilities (http://www.nsr.go.jp/archive/nsc/taishinkojo/pdf/gaiyou.pdf)

The Headquarters for Earthquake Research Promotion (2007) Report for "National Seismic Hazard Maps for Japan"

Tsuda, K., S. Dorjpalam, K. Dan, S. Ogawa, T. Watanabe, H. Uratani, and S. Iwase (2012) Dynamic Simulations for the Seismic Behavior on the Shallow Part of the Fault Plane in the Subduction Zone during Mega-Thrust Earthquakes(2), Abstract of Seismological Society of Japan, Fall meeting.

Yoshida, K., K. Miyakoshi., and K. Irikura (2011) Source process of the 2011 off the Pacific coast of Tohoku Earthquake inferred from waveform inversion with long-period strong-motion records, *Earth Planets Space,* **63**, 577-582.